

**Experiment no.:** HC-3014,      **Beamline:** ID 32,      **Dates:** 16.03.2017 – 22.03.2017

**Local contact:** Dr. Flora Yakhou-Harris,      **Shifts:** 18

### **Background and objective**

For this experiment we proposed to investigate the magnetisation dynamics within micro-scale magnetic elements by use of holography with extended reference by autocorrelation linear differential operator (HERALDO). The main objective was to obtain time-resolved images of the magnetic vortex cores gyration in “double Landau” states, induced by use of a magnetic pulse through a co-planar waveguide (CPW). Additionally, we wanted to image magnetisation dynamics of the domain walls and any effects leading to reversal of magnetic singularities, including polarisation of the cores and the ‘corners’ of the elements.

*\*The results of this work is currently being prepared for publication and are planned to be submitted later this month. The results of the previous experiment have now been published in Scientific Reports: ‘N. Bukin et al. Time-resolved imaging of magnetic vortex dynamics using holography with extended reference autocorrelation by linear differential operator, Scientific Reports, 6, 36307 (November 2016).*

### **Results and conclusions**

Figures 1, 2a and 2b depict the experimental setup and procedure used within this experiment. Time-resolution was achieved by using the standard stroboscopic pump-probe arrangement where the master clock of the synchrotron facility (probe) was used to trigger the magnetic (pump) RF pulse used to initiate vortex gyration. A delay is introduced between these pump and probe pulses which allows imaging the different phases of the samples internal magnetic state at regular intervals. The facility was running in 16 bunch mode with a probe pulse period of roughly 170 ns, allowing sufficient time for vortex gyration to dampen before the next pump/probe pulse. By using a relatively large RF pulse width of 30 ns allowed us to excite gyration on both the leading and trailing edge of the pulse whilst still leaving enough time between each pulse for sufficient dampening to occur and maintaining the confidence for identifying the exact position of the probe pulse within the pump pulse.

The samples used are shown in figure 1, 2c and 2d. It consists of a single column of magnetron sputtered Permalloy (Py) squares (2000 x 2000 x 80 nm) along the central signal line of an integrated gold CPW. The CPW was fabricated using the standard electron beam lithography, thermal evaporation and lift-off process with the following parameters: 4  $\mu\text{m}$  wide central signal line, 75 nm thick and 1  $\mu\text{m}$  separation from the 35  $\mu\text{m}$  ground tracks on either side of the signal line. These were chosen to suit the 50 ohm impedance of the signal generator and SMA cables used. The integrated CPW was connected via gold wire bonds to a standard CPW with an SMA connector. Figure 2d shows the position of the reference slit in the ground strip of the integrated CPW. The slit was milled through the entire sample stack (CPW/membrane/gold mask) via focussed ion beam (FIB) and were 6  $\mu\text{m}$  long and on average 30-40 nm wide. The slit width generally determines the intensity of the interference pattern and the overall resolution of the reconstructed image.

X-ray imaging was performed at 45° to the incident x-ray beam to obtain in-plane magnetic contrast within the sample. Figure 3 shows the field-dependence of the magnetic state within the Permalloy square. As was found previously (HC2117), the hysteresis properties of the relatively thick elements of this size lead to the Double-Landau state, with 7 domain structure. According to the

micromagnetic simulations, the dynamic behaviour of the system is determined by the interaction of the two cores, which are formed in the opposite (diagonal) closures of the system. When excited with a square pulse the gyration of the cores is heavily damped, and varies on the polarity of the cores. In the experiments, although we could easily create these states, their dynamic stability was really poor and in all trials after activation these states would eventually collapse into single Landau state. Further simulations verified that the stability of the double-Landau state is critically dependent on the thickness, and a more stable configuration would require a higher aspect ratio elements.

In further measurements, we have examined the dynamics of the 'extended' vortex system in a single Landau state. Again using a pulsed field excitation. This case is interesting because it has a structure reminiscent to 'half' of double-Landau. In order to create it, an external field was applied to displace the vortex from the equilibrium state (in the centre of the sample) towards one of the sides of the element. In the case of thin films ( $\sim 20$  nm), the vortex is usually annihilated, once the core is in close proximity to the edge. However, if the thickness of the sample is increased, it becomes favourable for the energy to keep the core in the sample. Only that in this case the core is becoming 'stretched' making it resembling a 180 degree (Bloch) domain. When excited with the external pulsed magnetic field, this domain wall starts a gyration motion. Figure 4 shows the experimental measurements of the stretched vortex excited with the pulsed field. From the coordinates of the edges of the domain wall, it can be seen that the both ends of the domain wall gyrate with a phase difference of 90 degrees, so that the length of the domain wall oscillates, analogous to a mechanical spring. This behaviour is well matched by the micromagnetic simulations, using the same parameters of the bias and the pulsed magnetic fields. Furthermore, investigating details of the structure of domain walls, the simulations show that the structure of the stretched vortex is non-uniform and has vortex formations on top and on bottom surface of the element. Figure 5 shows these results, together with a comparison to an equivalent element with lower thickness.

Finally, we carried out our preliminary experiments on time-resolved measurements of samples with coupled-Landau patterns (proposed in HC3310). Figure 6 shows examples of magnetic contrast imaged by HERALDO in two samples with different overlap of Landau patterns. Both samples, were initially exposed to the same bias field (0.5kOe), which was then removed and the remanent magnetisation and its dynamics imaged over a period of  $\sim 4$  ns from the start of the magnetic pulse. We found that because of the different overlap the ground state of the samples was completely different. Although, each sample had Landau patterns in both squares, the chirality of the domain closures was reversed. In one sample both vortices were with the same chirality, whereas in the other they were opposite to each other. This difference in chirality led to the fact that the coupling between the vortices had to be mediated via formation of an antivortex in the area of the vortices overlap. This has also meant that the dynamics of the coupled vortices was also entirely different. Figure 7 shows the preliminary results of vortex core tracks for the sample where the chirality of the vortex is reversed. These measurements show that the traces are antisymmetric and that the phase of the gyrations is shifted by 90 degrees. These results correlate well with the micromagnetic simulations.

A more detailed investigation of the coupled vortex gyration will be carried out in the proposed experiment HC3310. We will also explore more complex systems where we will attempt to couple more than two vortices and attempt their synchronised dynamic activation. The preliminary measurements reported here show that the proposed methods are well justified and we have the full confidence that the anticipated objectives will be completed.

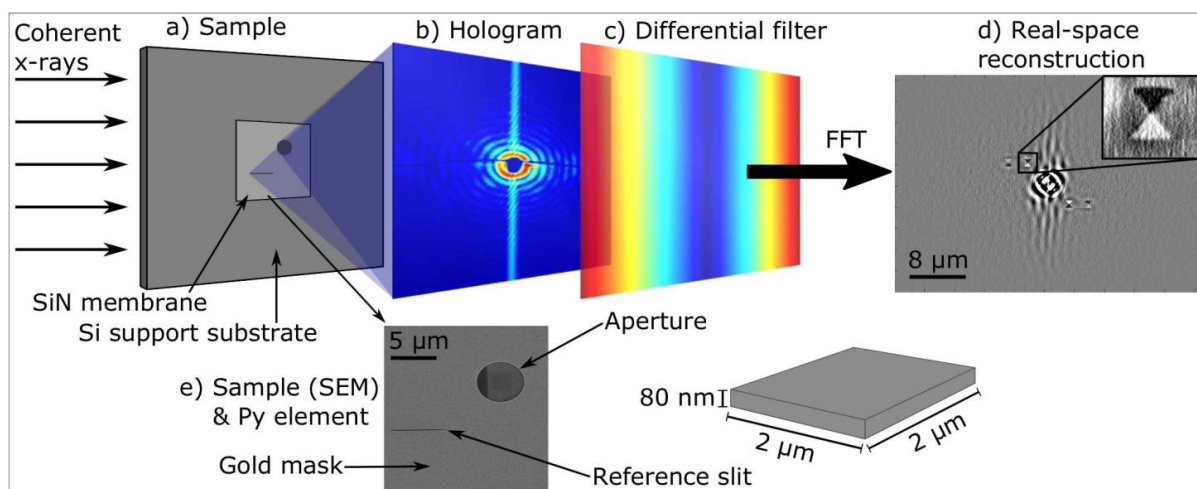


Figure 1: Schematics of the HERALDO setup and sample structure. (a) The SiN membrane containing the sample. The incident x-rays diffract at the aperture hole and the reference slit. (b) The interference between these two beams gives a hologram which is recorded on a CCD camera. (c) The intensity map of the differential filter, applied along the directional derivative of the x-rays from the reference slit. (d) The reconstructed image after fast Fourier transform (FFT) and polarisation analysis. Inset shows a close-up of the aperture with the magnetic contrast of the Py element. (e) Scanning electron microscope (SEM) image from the back side of the sample showing the aperture in the 600 nm gold layer together with the reference slit. The CPW with the square Py element can be seen in the aperture through the 200 nm SiN membrane on the front of the sample.

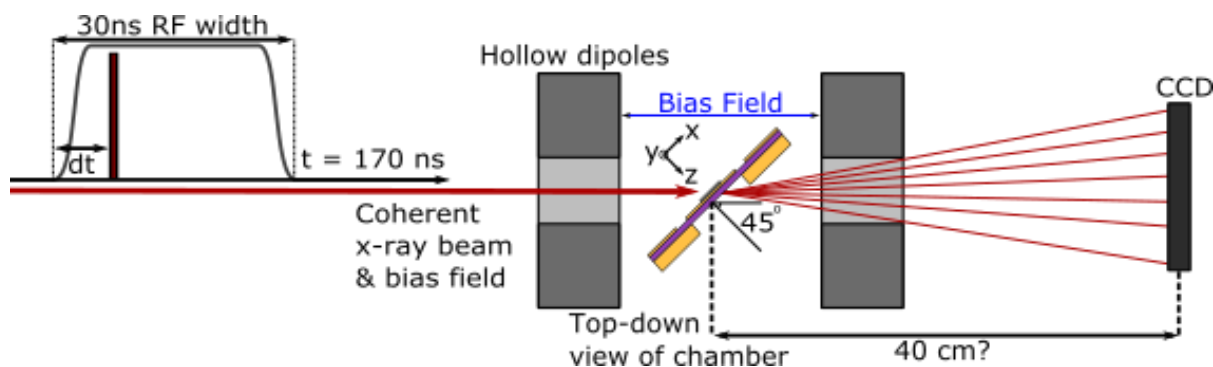


Figure 2: Experimental setup, sample orientation and time-structure of experiment. Pulsed pump-probe stroboscopic regime profile used based on facility master clock with a total period,  $t$ , of 170 ns. Sample in the chamber at  $45^\circ$  angle relative to the x-ray probe pulse and applied bias field, viewed top-down on the sample. X-rays diffract through the sample aperture and reference slit, interfere with each other to create the hologram which is then collected by the CCD roughly 40 cm

from the sample. Hollow dipoles in the chamber either side of the sample allow applying a bias field along the direction of x-ray beam propagation.

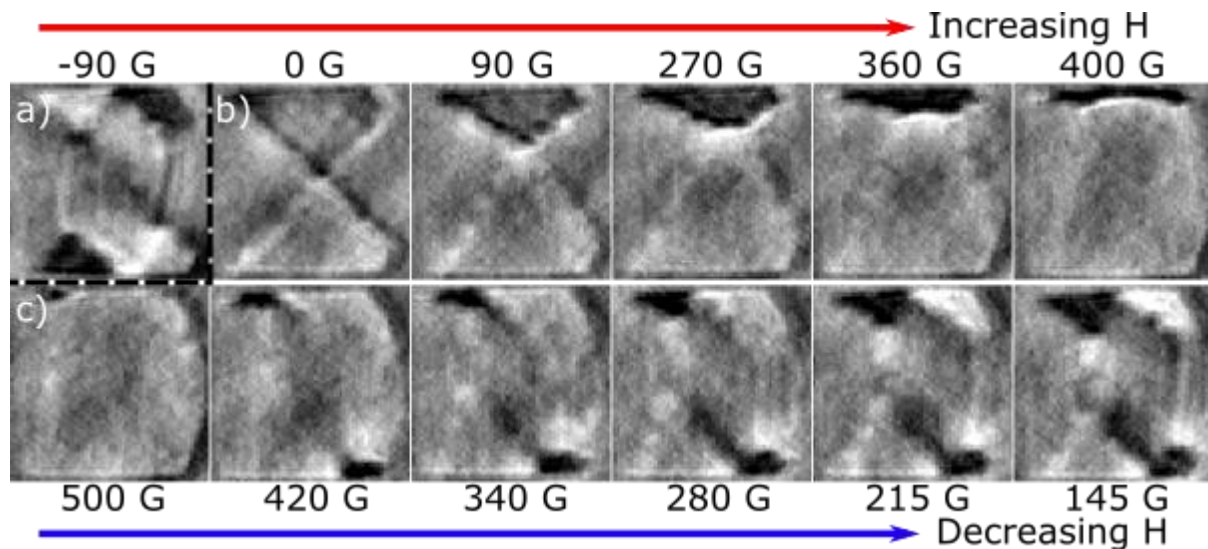


Figure 2: Field-dependence of magnetism within the sample. a) Shows the initial state formed when saturating the sample with a negative bias field and slowly stepping up to zero. b) Once the bias field reaches zero the Landau state reforms, the core then moves upwards with increasing field strength and eventually stretches until it exits the sample and is fully saturated in one direction. c) Upon reducing the applied field strength a 2-vortex (a.k.a 7-domain) state is slowly formed. This state is reproducible as we repeated this hysteresis multiple times and every time this state was reformed.

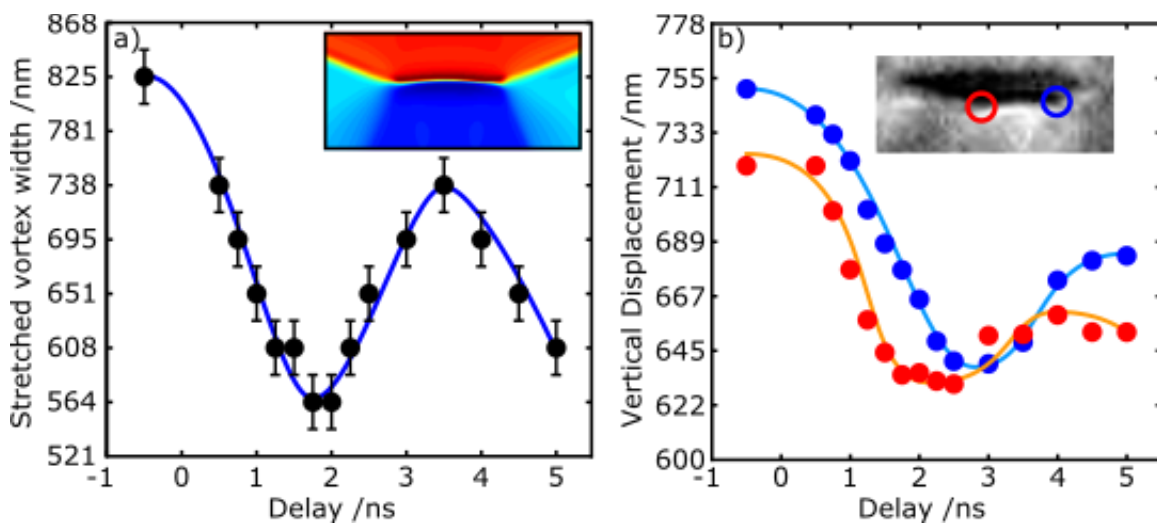


Figure 4: Width a) and vertical displacement b) of stretched vortex seen with 300 G bias field relative to the delay time used between the RF and x-ray pulses. The width in a) was calculated by counting the number of pixels above a certain intensity from one end to the other to calculate the length of the region, the black line being a guide to eye for the data. The vertical displacement in b) was calculated by taking an average intensity value for a width of 3 pixels through the last pixel on each end of the stretched vortex and finding the region where it passed through zero. Light blue/orange lines are a guide to eye for the blue/red data respectively. Insert shows which ends of the stretched region the data corresponds to.

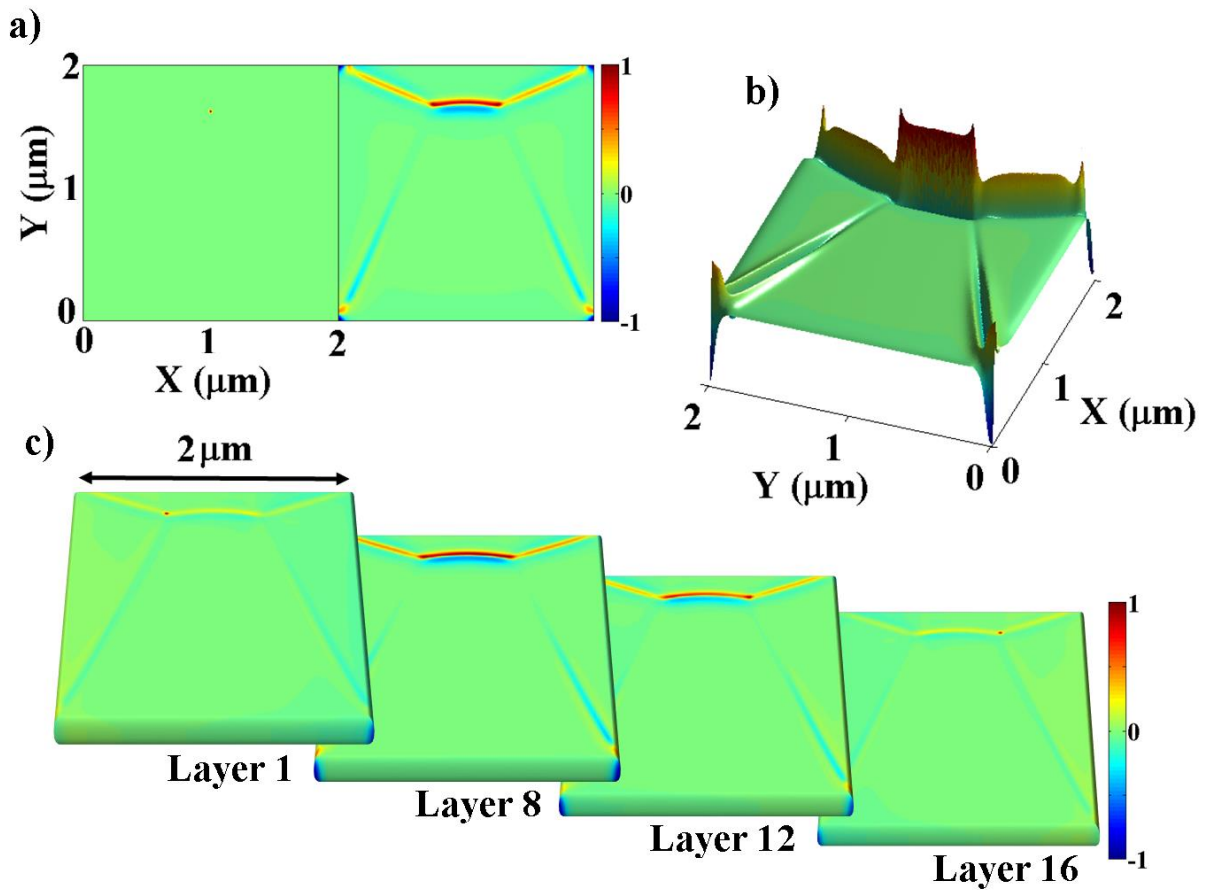


Figure 5: Stretched vortex core in biased magnetic field. a) Comparison between the domain structure of 20nm (left pane) and 80nm (right pane) thick elements in 300 Oe bias magnetic field. For 20 nm film the vortex core is preserved and displaced towards the top edge, for 80nm film the core is 'stretched' into domain wall. b) Surface plot of perpendicular magnetisation component of the 'stretched' vortex. c) the magnetisation structure of different layers of the element. Top and bottom layers exhibit magnetic vortices on the edges of the domain wall.

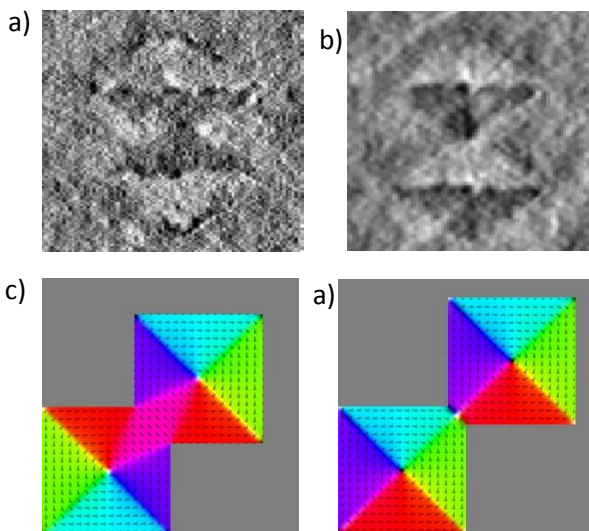


Figure 6: Coupled Landau states: imaged with x-rays at 20 degrees out-of-plane in the sample with vortices of opposite chirality (a) and in the sample with vortices of the same chirality (b). Similar configurations produced by the micromagnetic simulations (c,d). The coupling in the second case is via formation of an anti-vortex at the point of the squares overlap. The vortex cores are seen as black spots in both type of structures. The in-plane contrast is not well seen because the x-ray beam is mainly perpendicular to the surface.

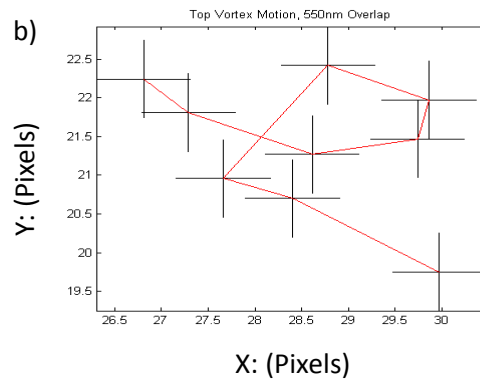
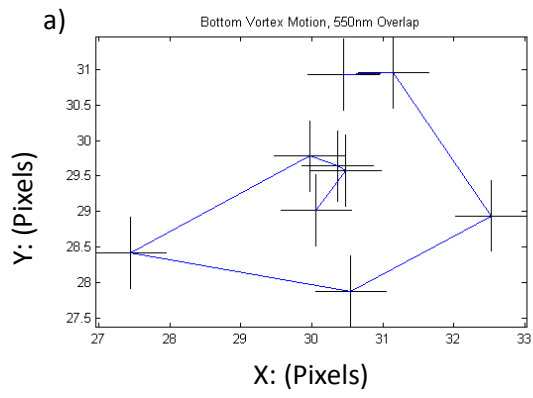


Figure 7: Vortex core traces after activation with a pulsed magnetic field for a sample with 550nm overlap. a) bottom vortex pattern b) top vortex pattern.